Linear stability and transient growth in driven contact lines

Andrea L. Bertozzi[a)]
Duke University, Department of Mathematics, Durham, North Carolina 27708

Michael P. Brenner[b)]
Department of Mathematics, MIT, Cambridge, Massachusetts 02139

(Received 17 January 1996; accepted 12 November 1996)

Fluid flowing down an inclined plane commonly exhibits a fingering instability in which the contact line corrugates. We show that below a critical inclination angle the base state before the instability is linearly stable. Several recent experiments explore inclination angles below this critical angle, yet all clearly show the fingering instability. We explain this paradox by showing that regardless of the long time linear stability of the front, microscopic scale perturbations at the contact line grow on a transient time scale to a size comparable with the macroscopic structure of the front. This amplification is sufficient to excite nonlinearities and thus initiate finger formation. The amplification is a result of the well-known singular dependence of the macroscopic profiles on the microscopic length scale near the contact line. Implications for other types of forced contact lines are discussed. © *1997 American Institute of Physics.* [S1070-6631(97)01103-3]

I. INTRODUCTION

Spreading viscous films have applications ranging from microchip fabrication to tertiary oil recovery. In the absence of forces, it is well known that the flow is perfectly stable.[1–5] However, as first appreciated by Huppert,[6] when a liquid film is driven by a constant force, the interface breaks into fingers. Since Huppert's initial experiments on fluid dripping down an inclined plane, studies have focused on more features of the inclined plane[7–9] as well as other experimental configurations, such as spin coating[10,11] and Marangoni forcing.[12,13]

The mechanism for the instability involves a subtle interplay between the fluid far from the front, where surface tension is irrelevant, and the fluid near the contact line, where surface tension dominates. In his original work,[6] Huppert characterized the flow far from the front. Troian *et al.*[14] and Hocking[15] first described the surface tension dominated region; Moriarty, Schwartz, and Tuck[16] and Goodwin and Homsy[17] provided more detailed descriptions. Numerical simulations by Schwartz revealed the fact that surface tension effects control the instability.[18] Troian *et al.*[14] presented a theoretical mechanism for the instability. They pointed out that the base state before the instability has, near the contact line, a thick ''bump'' that is responsible for the linear instability. By performing an analysis of the base state for fluid dripping down a vertical wall, they found a finite-wavelength most unstable mode and corresponding growth rate. The most unstable mode has a wavelength that is approximately three times the width W of the bump. Hocking and Miksis made similar calculations for the stability of a ridge.[19] Spaid and Homsy recently analyzed the mechanism for the instability,[20] and demonstrated that the dominant effect is that, under the action of a constant body force, thicker films have less resistance than thinner films.

All of the aforementioned experimental configurations have been compared with linear theory. Photographs of the experiment easily yield the finger wavelength while measurements of the finger length as a function of time give the growth rate.[9,13] For fluid dripping down an inclined plane, de Bruyn[9] finds qualitative agreement with the theoretical predictions. When his data for finger length as a function of time are scaled by the characteristic length scales of the base state proposed by Troian *et al.*,[14] the finger length grows exponentially in time, although the growth rate is about one fifth the predicted value. Furthermore, the average wavelength of the patterns is roughly 50 percent smaller than the predicted most unstable mode. Another complication is that the experiments often show an irregular fingering pattern, with the wavelengths of successive fingers differing by as much as 25 percent across the pattern. Frayasse and Homsy[11] compared data from centrifugal spreading with the theory, with better agreement: both the growth rates of the fingers and the average wavelength agree with theoretical predictions quite well. Finally, for thermally forced fingers Brzoska, Brochard-Wyart, and Rondelez[13] found good agreement.

We present several reasons for the discrepancy between the theoretical predictions and the experiment for flow down an inclined plane. First, when the plane is inclined to the vertical there is a component of gravity perpendicular to the incline plane. Our calculations show that this additional force has significant consequences for the shape and stability of the front. Below a critical inclination angle α^*, the bump in the profile completely *vanishes*, and the front is linearly stable. The critical inclination angle α^* is above the smallest values used in de Bruyn's experiments and also in the initial experiments of Huppert. Thus instability and finger growth seem to occur in experiments even though the front is linearly stable. This additional force stabilizing the front is not important in centrifugal spreading at the high rotation rates typically used in experiments, and also is not present in the thermally forced experiments of Brzoska. For centrifugal spreading, there is a critical rotation rate below which centrifugal spreading is also linearly stable. Experiments on in-

a)Electronic mail: bertozzi@math.duke.edu
b)Electronic mail: brenner@math.mit.edu

clined planes show instability even for very small inclination angles.

The second important factor is that regardless of whether the front is linearly stable, there is significant *transient* growth over the typical time of the experiment. The mechanism for transient growth stems from the singular dependence of the base state on the microscopic length scale at the contact line. The amount of transient growth depends inversely on the microscopic scale (typically 10^{-3}–10^{-4} times the macroscopic thickness of the film) at the contact line, so that perturbations of all wave numbers can grow by a factor of 10^3-10^4 during an experimental time scale. Transient amplification of small perturbations near the contact line occurs both above and below the critical inclination angle for linear stability.

A final feature is that both the linear instability at large inclination angles and the transient growth modulate the thickness of the front without corrugating the contact line. In order to cause finger growth, nonlinearities are necessary;[21] this requires that the time scale of nonlinear effects is less than the time scale for modulating the thickness of the front. Applying this criterion leads to the result that there is a *second* critical inclination angle depending on the contact angle of the fluid below which the profile is both linearly stable and the nonlinear finger formation mechanism does not occur on a time scale that is fast enough to amplify transient growth. In this regime, no fingering occurs.

The organization of this paper is as follows. Section II reviews the dynamic equations describing fluid flow down an inclined plane (following Troian *et al.*[14]) and shows how the inclination angle modifies the shape of these traveling waves. Section III considers the linear stability analysis of these traveling wave solutions as a function of inclination angle. As expected, when the bump in the profile vanishes, the profiles are linearly stable. Section IV discusses transient growth. Section V reviews conclusions and predictions.

II. MATHEMATICAL FORMULATION

We study the evolution of fluid, released at the top of an inclined plane, as it drips down the incline. The fluid/air/solid contact line is initially straight, but may form fingers as the interface evolves. First we discuss the lubrication approximation for such a setup, including the different regions of interest and their length and time scales. Then we discuss the particular contact line model chosen here, the ''traveling wave solutions'' in this model and a comparison of the parameters in the model with actual experiments.

A. The lubrication approximation

The standard mathematical formulation for such wetting flows is the lubrication approximation:[22] by depth averaging the velocity field of the liquid over the thickness of the film, the Stokes equations reduce to a more tractable partial differential equation for the thickness of the film.

If the film thickness is $h(x,y,t)$, the velocity $V(x,t)$ is

$$3\eta V(x,y,t) = -h^2\nabla p + \rho g \sin(\alpha) h^2 \mathbf{x}, \tag{1}$$

where η is the viscosity, p the internal pressure, ρ the fluid density, and g the gravitational acceleration. The pressure is

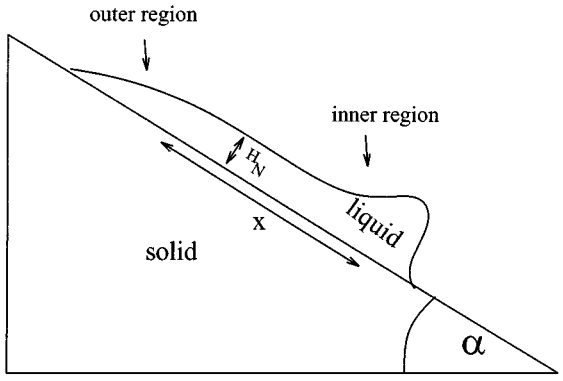

FIG. 1. Schematic diagram of the problem.

$$p(x,y,t) = -\gamma\nabla^2 h + \rho g \cos(\alpha) h, \tag{2}$$

where γ is the liquid surface tension. Conservation of mass then gives an evolution equation for the thin film height,

$$3\eta\frac{dh}{dt} + \nabla\cdot(\gamma h^3 \nabla\nabla^2 h - \rho g \cos(\alpha) h^3 \nabla h) + \rho g \sin(\alpha)(h^3)_x = 0. \tag{3}$$

After the flow begins, the height profile develops two regions (see Fig. 1). The *outer region*, far from the contact line, is dominated by the component of gravity, $\rho g \sin\alpha$, parallel to the surface. The solution in this region can be described by a similarity solution of Huppert,[6]

$$h(x,t) = \sqrt{\frac{\eta x}{\rho g \sin\alpha t}}. \tag{4}$$

Conservation of mass implies that the length of this region increases as $x_N \sim t^{1/3}$ and the thickness decreases as $H_N \sim t^{-1/3}$.

Near x_N, the edge of the outer region, the profile is smoothed by surface tension. Troian *et al.*[14] proposed a quasi-steady approximation in which the outer solution provides boundary conditions for the flow in this *inner region*. Troian *et al.*[14] and Hocking[15] use these boundary conditions to set the scale for the flow near the contact line. The appropriate scalings are

$$\begin{aligned} h &= \overline{h} H_N, \\ (x,y) &= (\overline{x}\ell, \overline{y}\ell), \\ t &= \overline{t}(\ell/U). \end{aligned} \tag{5}$$

Here, $\ell = H_N/(3\mathrm{Ca})^{1/3}$, where $\mathrm{Ca} = \mu U/\gamma$ is the capillary number. When expressed in terms of these units, the height and width of the base profile remain nearly constant in time. With these rescalings (dropping the bars), Eq. (3) becomes

$$h_t + (h^3)_x + \nabla\cdot(h^3\nabla\nabla^2 h - \cot(\alpha)(3\mathrm{Ca})^{1/3} h^3 \nabla h) = 0. \tag{6}$$

In the forthcoming analysis, we define $D(\alpha) = \cot(\alpha) \times (3\mathrm{Ca})^{1/3}$. The importance of this quantity was noted by Goodwin and Homsy[17] who considered the distinguished limit $\mathrm{Ca}\to 0$, $D\to 1$.

It is useful to estimate the capillary number of the flow as a function of the inclination angle. The flow field away from the contact line determines the characteristic velocity scale. If L is the characteristic span-wise variation of the film, then the characteristic time scale τ of the flow in the outer region is

$$\tau = \frac{3\eta L}{\rho g \sin(\alpha) H_N^2},$$

so that the velocity $U \sim L/\tau$, and the capillary number is approximately

$$\mathrm{Ca} = \frac{\eta U}{\gamma} \approx \frac{\rho g \sin(\alpha) H_N^2}{3\gamma} = \frac{\tan(\alpha)}{3}\left(\frac{H_N}{\ell_{\mathrm{cap}}}\right)^2, \tag{7}$$

where $\ell_{\mathrm{cap}} = \sqrt{\gamma/(\rho g \cos(\alpha))}$ is the capillary length. Note that the capillary number is weakly time dependent due to the time dependence of H_N.

B. Contact line model

The analysis in this paper addresses the case of completely wetting fluids. Even in this case, the boundary condition at the contact line is a subject of debate.[23,24,2] In this paper we use the model proposed by Troian *et al.*[14] To avoid confusion we briefly justify the model and point out its limitations. For completely wetting fluids (with zero equilibrium contact angle), the only dependence of the profile far from the contact line on the microscopic physics near the contact line is a *logarithmic* dependence on the microscopic length scale.[25,26,2] No other microscopic parameter appears in the outer flow field. This result was first established by Dussan[26] and later discussed through general scaling arguments by de Gennes.[2] The logarithmic dependence on the microscopic scale arises in relating the velocity U of the front to the macroscopic contact angle θ, through Tanner's law

$$\gamma\theta^2 = \eta U \frac{(\log(1/b))}{\theta}, \tag{8}$$

where b is the ratio of the microscopic to macroscopic length scales. This formula represents the balance between surface energy and energy dissipation in a moving wedge. The logarithm arises from the divergence of the energy dissipation at the contact line.[26]

Realistically modeling the contact line is extremely difficult. The fact that the macroscopic flow depends on contact-line physics only through Eq. (8) allows an enormous simplification: it is legitimate to use *any* model of the microscopic physics near the contact line as long as it leads to the macroscopic spreading law Eq. (8). The simplest such model, proposed by Troian *et al.* in Ref. 14, gives the microscopic physics as a thin film of thickness b preceding the front (see Fig. 2). Although this thin film model does not accurately reproduce the actual microscopic physics near the contact line, it introduces the microscopic scale b into the macroscopic flow field in the required manner. The length scale b does have physical significance, and represents the characteristic scale of the microscopic physics in a particular experiment. For spreading on a rough surface, this length scale is just the scale of surface roughness. For spreading on smooth surfaces, b would be set by van der Waals interactions.

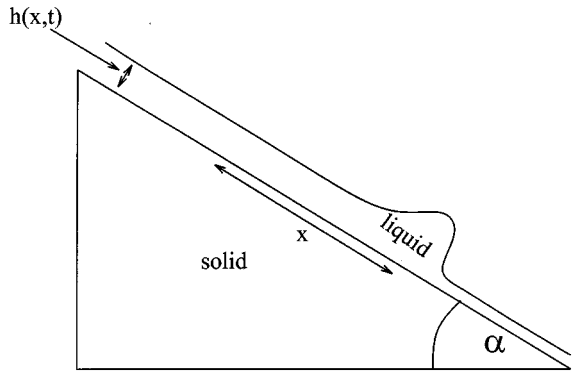

FIG. 2. Schematic diagram of the model.

C. Traveling wave solutions

The base state before the instability[14,15] is a traveling wave solution $h(x,y,t) = h_0(x - Ut)$ of (6). The function $h_0(x)$ satisfies

$$-Uh_0 + (h_0{}^3 h_{0xxx} - D(\alpha) h_0{}^3 h_{0x}) + h_0{}^3 = d, \tag{9}$$

where d is a constant of integration, and

$$D(\alpha) = \cot(\alpha)(3\mathrm{Ca})^{1/3} = \left(\frac{\cot(\alpha) H_N}{\ell_{\mathrm{cap}}}\right)^{2/3}. \tag{10}$$

Matching the front onto the rest of the solution specifies the integration constant d and the velocity U of the traveling wave.[16] As $x \to -\infty$, the front matches onto $h_0 \to 1$. As $x \to \infty$, the front must match onto the contact line. These two matching conditions fix both U and d to be

$$U = \frac{1-b^3}{1-b}, \quad d = -b\frac{1-b^2}{1-b},$$

which uniquely fix the traveling wave solution.

Given b and D, Eq. (9) can be solved for the shape of this solution. The first graph in Fig. 3 shows for different b the profiles corresponding to $D = 0$, in agreement with the results of Troian *et al.*[14] These profiles all have a distinct bump at the contact line. As mentioned above, the length scale of the linear instability is given by the characteristic width of this bump. The second graph in Fig. 3 shows profiles when $D = 2.5$. Here the situation is different: For all profiles, the size of the bump is substantially diminished. At $b = 0.1$, it has essentially disappeared. Increasing D slightly higher further diminishes the size of the bump. As the last graph (lower left) in Fig. 3 shows, for $D = 5$, the bump for $b = 0.01$ has completely disappeared. A slight bump remains for $b = 0.001$.

The height of the bump is a strong function of D and b. Since the bump height is the crucial parameter for determining whether the profile is stable or unstable, we show in Fig. 4 the height of the bump as a function of these parameters.

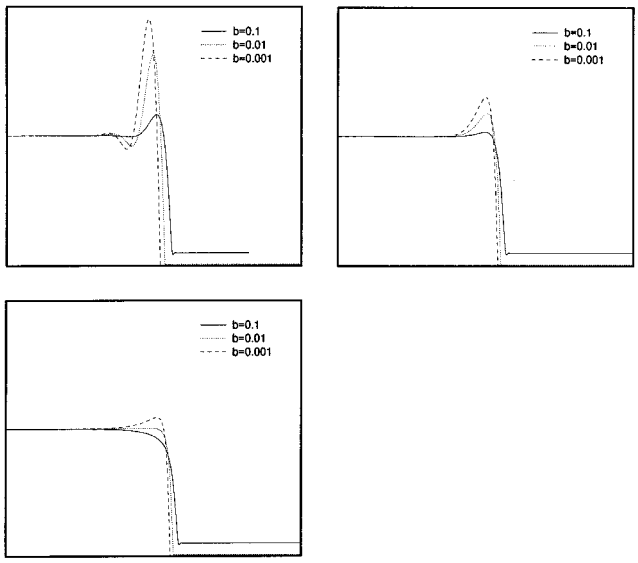

FIG. 3. Profiles for $b=0.1$, 0.01, and 0.001. The maximum thickness of the bump is a logarithmic function of b. The first graph shows the case $D=0$, the second $D=2.5$ and the third $D=5$. Note that in each successive graph, the heights of the bumps are substantially diminished. For the case $D=5$ there is no bump in the $b=0.1$ and $b=0.01$ profiles. For $b=0.001$ there is a very slight bump.

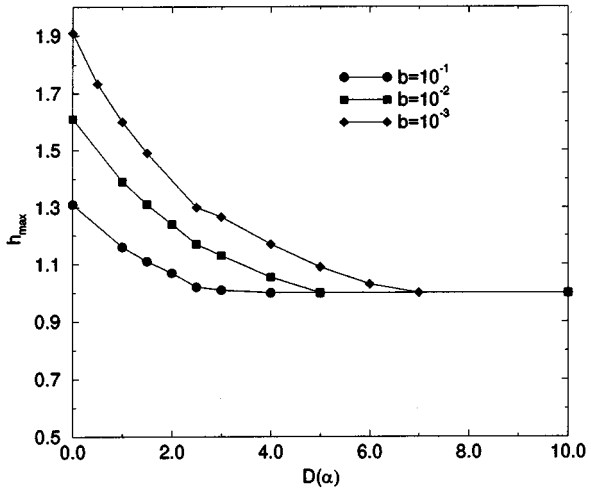

FIG. 4. Maximum height of the profiles as a function of D for different values of b. When the maximum height is near 1, there is no longer a bump in the profile.

For each value of b there is a critical value of D for which the bump completely disappears. We verify below that when the bump disappears, the front is linearly stable.

The traveling wave solutions have a characteristic scale W in the x direction over which the thickness of the film decays. The scale W depends strongly the inclination angle. For α near 90 degrees, W is of order ℓ, independent of α when expressed in the units of Eq. (5). When the gravitational flattening term is important the characteristic width of the profile is *not* given by the scalings of Eq. (5), but instead by

$$W \sim D(\alpha)\ell = H_N \cot(\alpha).$$

At high D the decay of the front is much more gradual than at $D=0$. However, it is important to note that close enough to the edge there is *always* a region of size ℓ where surface tension is important.

By solving the full Stokes equations, Goodwin and Homsy[17] made extensive calculations of the profiles at small inclination angles. Their calculations demonstrate that the size of the bump decreases with decreasing inclination angle. They also discuss the dependence of the size of the bump on the contact angle boundary condition. The latter dependence is outside the focus of this paper, since we consider only completely wetting fluids.

D. Comparison with experiments

Given the strong dependence of the shape of the profile on the value of D, it is of interest to know the value of D in the experiments. Combining formulas (7) and (10) shows that at small angles, $D(\alpha) \sim \alpha^{-2/3}$. The fact that $D(\alpha)$ becomes large at low inclination angles was emphasized by de Bruyn.[9] By measuring the thickness H_N of the film before the instability sets in, he deduced D and showed that D diverges at low inclination angles;[27] even at the highest inclination angles D is still order one.

For each value of b, there is a critical value of D in (9) above which the bump in the profile completely disappears. Using the parameters given for de Bruyn's experiments ($\gamma=19.4$ dyn/cm, $\eta=0.525$ g/cm/s and $H_N=0.3$ cm) yields $D(\alpha)=1.64(\sin(\alpha))^{1/3}\cot(\alpha)$. This function is plotted in Fig. 5.

A typical experimental surface has microscopic imperfections on the scale of μm, suggesting $b \sim 10^{-3}-10^{-4}$. The calculations shown in Fig. 4 indicate that D must be at least in the range 5–8 in order to suppress the bump. The corresponding critical angle is around $\alpha^* \approx$ 5–10 degrees. The inclination angles explored in de Bruyn's experiments are in the range 2–20 degrees, so at the smallest angles in the

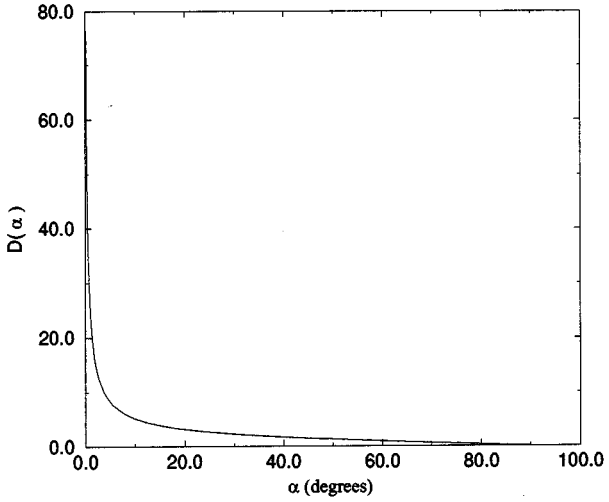

FIG. 5. $D(\alpha)$ as a function of α for the parameter values of de Bruyn's experiments. Note that D diverges as $\alpha^{-2/3}$ at small angles.

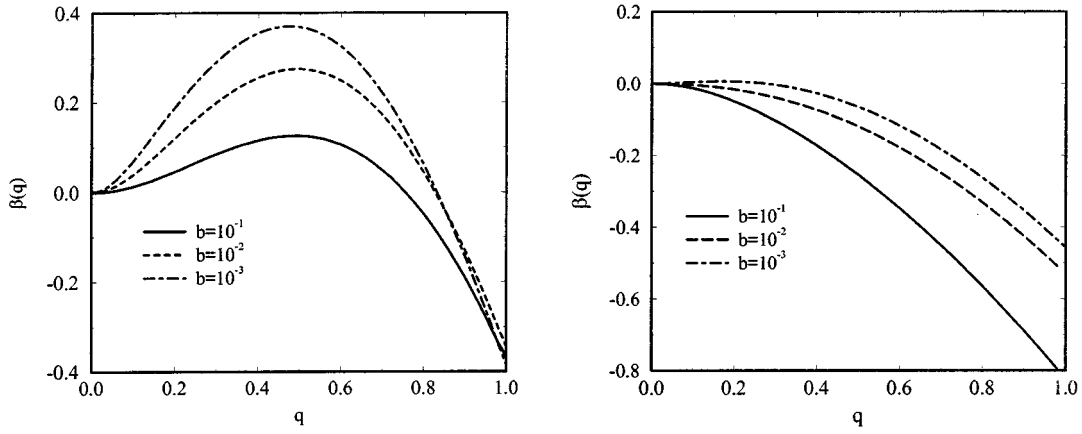

FIG. 6. The growth rate $\beta(q)$ computed from the long time behavior of solutions of the linear PDE (12) with $D(\alpha)=0$ (top) and $D(\alpha)=5$ (bottom).

experiment the initial profile should not have a bump. For the original experiments of Huppert, the inclination angle is around 12 degrees, indicating a slight bump.

In an actual experiment D is *time dependent*; in the above analysis, the quasi-steady approximation assumes it is constant. We discuss the consequences of this assumption at the end of Sec. III.

III. LINEAR STABILITY ANALYSIS

The traditional approach to hydrodynamic stability is via a linearization of the equation about a steady solution followed by an eigenvalue analysis of the linearized problem. In this section we compute the largest eigenvalue associated with the linearization of (6) about the traveling wave solution h_0 to (9) and discuss the role of the gravitational force normal to the inclined plane. We show that there is a discrepancy between experimental results and stability predictions via eigenvalue analysis. In the next section we show that an eigenvalue analysis does not accurately capture the relevant dynamics of the linearization.

Following Troian *et al.*,[14] we use a reference frame traveling with the speed of the traveling wave $U=1+b+b^2$. Consider a perturbation, $\epsilon g(x,y,t)$, to the front h_0. We think of g as $O(1)$ and $\epsilon \ll 1$. Later we discuss the relevant size of ϵ for physical experiments. Plugging $h=h_0+\epsilon g(x,y,t)$ into (6) and saving only those terms that are $O(\epsilon)$, to first order in ϵ the equation for the perturbation profile g is

$$g_t+\nabla\cdot(3{h_0}^2 g(\nabla\nabla^2 h_0-D(\alpha)\nabla h_0))+\nabla\cdot({h_0}^3(\nabla\nabla^2 g - D(\alpha)\nabla g))+3({h_0}^2 g)_x-Ug_x=0. \quad (11)$$

The eigenfunctions and eigenvalues of solutions to (11) determine the classical linear stability. Since the steady solution, h_0, does not depend on the transverse variable y, Eq. (11) can be Fourier transformed in y

$$g(x,q)_t+\partial_x(3{h_0}^2 g(\partial_x^3 h_0-D(\alpha)\partial_x h_0))+\partial_x({h_0}^3(\partial_x^3 g - D(\alpha)\partial_x g))-q^2 h_0^3 g_{xx}+D(\alpha)q^2 h_0^3 g - q^2\partial_x(h_0^3\partial_x g)+q^4 h_0^3 g+3(h_0^2 g)_x-Ug_x=0. \quad (12)$$

Note that if h_0 were constant, Eq. (12) would have no unstable modes. Thus the linear instability results from the complex structure of h_0.

Troian *et al.*[14] calculated the growth rate for small q: If $g(x,q)=e^{\beta t}\varphi(x,q)$, the spatial dependence $\varphi(x)\approx h_{0x}$ for sufficiently long wavelength disturbances (since h_{0x} is the marginal translation mode). Then to leading order in q^2, the growth rate is

$$\beta(q)=\frac{q^2}{1-b}\int_{-\infty}^{\infty}(h_0-1)(h_0-b)(h_0+1+b)dx. \quad (13)$$

This equation holds even when D is nonzero.

The most important feature of Eq. (13) is that if $h_0<1$, then $\beta(q)<0$ at long wavelengths. For β to be positive, h_0 must be greater than one in a large enough region that the positive portion of the above integral cancels out the negative portion. Thus, for the profile to be linearly unstable the bump must have a finite size.

Now we determine the eigenvalues $\beta(q)$ as a function of q by solving the full linear PDE (12) numerically on a suitably large domain. For each q, we start with a generic initial condition, examine the long time behavior of the solutions to Eq. (12), and extract the exponential growth (decay) rate. The numerical scheme is a standard implicit finite-difference scheme (see e.g., Ref. 28); the only complication is that for small b, it is necessary to use a nonuniform mesh with refinement at the apparent contact line in order to completely resolve the unperturbed profile h_0. Figure 6 shows $\beta(q)$ for several small values of b for both $D(\alpha)=0$ and $D(\alpha)=5$.

The growth rate curve shown in Fig. 6 for $D=0$ agrees with the computations of Troian *et al.*[14] However, a moderate value of $D(\alpha)$ modifies the growth rate considerably; the profile is linearly stable when b is larger than a critical value $b^*(\alpha)$ depending on the inclination angle. As suggested by both intuitive reasoning and the long wavelength calculation discussed above, linear stability corresponds to the disappearance of the bump in the profiles.

The linear growth rates in Fig. 6 suggest a paradox: the bump responsible for the linear instability disappears at the small inclination angles of the experiment, but the experiment still shows that the interface destabilizes. What could

be the reason for this discrepancy? We describe below three different possibilities, the last of which we believe to be the most relevant. We elaborate on this point in subsequent sections.

One scenario[29,18] uses the breakdown of the quasi-static approximation to explain the change in stability: at early times D may be of significant size, however the thinning of the film described in (4) causes D to decrease over time. In this picture the instability occurs as soon as D is small enough so that the profile is linearly unstable. At small inclination angles, the condition $D\sim 1$ is equivalent to the film thickness satisfying $H_N \sim \alpha \ell_{cap}$. The capillary length is typically a few millimeters; thus when $\alpha = 3$ degrees, (the smallest angle in de Bruyn's experiments), the film thickness would have to be smaller than ≈ 0.1 mm for D to be in the unstable regime. The measured thickness in de Bruyn's experiments,[9] are 0.3 cm, about a factor of ten larger than this threshold. Thus, the hypothesis that D decreases until the film becomes linearly unstable seems insufficient to explain the instability in de Bruyn's experiments; however, a different experimental setup might attain $D\sim 1$ at very low inclination angles by using extremely thin films.

Two other scenarios are motivated by similar problems arising in the transition to turbulence in shear flows. In this situation, an instability is observed at a Reynolds numbers where the base state is linearly stable. One explanation, due to Landau,[30] describes the instability as weakly nonlinear and represents a finite amplitude instability to a nearby nonlinear state. Another explanation involves transient growth, in solutions to the linearized equations, that triggers the nonlinear instability.[31–37]

Below, we demonstrate that there is in fact significant transient growth in Eq. (12) due to the singular dependence of the solution on the microscopic length scale b at the contact line. The transient growth occurs *regardless* of whether there is bump in the profile. We argue that this last scenario is the most natural to explain the discrepancy between the growth rates in Fig. 6 and experiments.

IV. TRANSIENT GROWTH

In the previous section we performed a classical hydrodynamic stability analysis, namely linearization of the equation and computation of most unstable eigenvalues. Recently, it has been pointed out that for certain problems this approach can give results that do not correlate with experiments, not because of the failure of the linearization, but because of the failure of the eigenvalue analysis.[31–36] Indeed, the eigenvalues predict the long time state of the linearized system. And, when the associated eigenfunctions are all orthogonal the eigenvalues accurately capture the short time effects as well. However, in the case of a strongly nonnormal system, in which eigenfunctions are closely aligned, transient effects can occur that mask, on an intermediate time scale, the behavior predicted by the eigenvalues. The linearized equation accurately approximates the evolution of a perturbation of the steady state as long as it remains small. In the case of nonnormal operators, a solution to the linearized equation may grow by orders of magnitude on a transient time scale, even though all the underlying eigenvalues predict stability. This kind of growth may cause an initially small perturbation to reach an order one size on a transient time scale, exciting nonlinearities and causing an observable instability.

The goal of this section is to illustrate that regardless of the size of the bump in the front h_0 (hence regardless of the eigenvalues of the linearization), solutions of (12) grow by a factor of $1/b$ on a transient timescale, that is by a factor that scales inversely with the microscopic length scale. Since in experiments b typically is of order $10^{-3}-10^{-4}$, this effect is considerable. It is sufficient to explain instability where eigenvalue analysis fails, if it causes a perturbation to grow to size $O(1)$, that is if the initial perturbation size ϵ satisfies $\epsilon = O(b)$ where $b \ll 1$. This situation is in fact expected, e.g., in the case of surface roughness, the size of the roughness determines both the microscopic scale for the model and the size of the noise. We also note that, as shown in Ref. 34, transient growth of a smaller magnitude than the inverse of the characteristic size of the noise can sometimes still ultimately lead to $O(1)$ effects via a ''bootstrapping'' mechanism involving the nonlinearity.

Before presenting the numerical results showing transient amplification of solutions to the linearized equation (12), we present a heuristic argument, based on the shape of the capillary profile, for why we might expect a $1/b$ scaling for the amplification factor.

A. Contact lines are amplifiers

We give a general argument that demonstrates that contact lines are amplifiers: namely, small perturbations to the interface in the vicinity of a contact line cause much larger perturbations to the outer flow field.

Consider a perturbation of size ϵ in the microscopic region near the contact line. The response of the outer flow field to this perturbation can be considered within our simplified model of the contact line, by studying a perturbation of size ϵ to the thin film region ahead of the front. The major effect of this perturbation will be to change the local microscopic length scale from $b \to b+\epsilon$. In an experiment, ϵ will be on the order of b, since it typically represents fluctuations in the microstructure. As argued above in section II, the leading order dependence of the outer flow field on the microscopic length scale is exactly captured by the simplified contact line model; hence, the response of the outer flow field to the perturbation will be captured by our model. Figure 7 shows a sketch of such a perturbation to the model.

The crucial point in considering how this perturbation effects the outer flow field is that the maximum height of the thick film depends in a singular way on microscopic scale. This logarithmic dependence is demonstrated in Fig. 3: the profile away from the contact line (e.g., the maximum thickness of the film) is a logarithmic function of b. The reason for this logarithmic dependence was given by Dussan and Davis,[25] Dussan,[26] and de Gennes,[2] who showed that it generically arises from matching the behavior near the contact line (where $h \sim x(\log(x/b))^{1/3}$) to the thick film. Placing a perturbation of size ϵ on the thin film changes the front height from $b \to b+\epsilon$. This causes the outer solution (for example, the maximum height of the film) to become

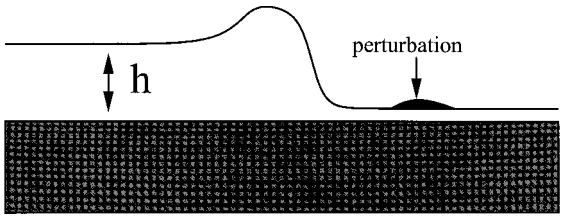

FIG. 7. Sketch of a type of perturbation to the profile that can cause transient growth.

$$h_{\max}(b+\epsilon)\sim f\left(\log\left(\frac{1}{b(1+\epsilon/b)}\right)\right)\approx f\left(\log\left(\frac{1}{b}\right)\right)$$
$$-f'\left(\log\left(\frac{1}{b}\right)\right)\frac{\epsilon}{b}\sim h_{\max}(b)+O(\epsilon/b).$$

Thus, the contact line *amplifies* the perturbation by a factor

$$\frac{\Delta h_{\max}}{\epsilon}\sim\frac{1}{b}.$$

For experiments with $b=10^{-3}$–10^{-4}, growth by a factor of 10^3–10^4 can occur. Since we expect the scale of perturbations to be on the order of size of the microstructure (that is the size of b), this means that they will amplify to cause order one changes in the front. The time scale of this amplification is the amount of time it takes for the traveling wave to pass over the perturbation. Note that this same argument holds if the perturbation at the contact line varies with wavelength much larger than W.

Now we verify the existence of transient growth in Eq. (12) by explicit computation. We consider $b=0.1$ and $D(\alpha)=0$, with an initial perturbation $g=G(y)\,\varphi(x)\sin(x/3)$, where φ is a cutoff function localized around the downslope of the front and contact line. We compute the solution of the linearized Eq. (12) for different values of q. Figure 8 depicts the ratio

$$R(t)=\max_x|g(x,t)|/\max_x|g(x,0)|$$

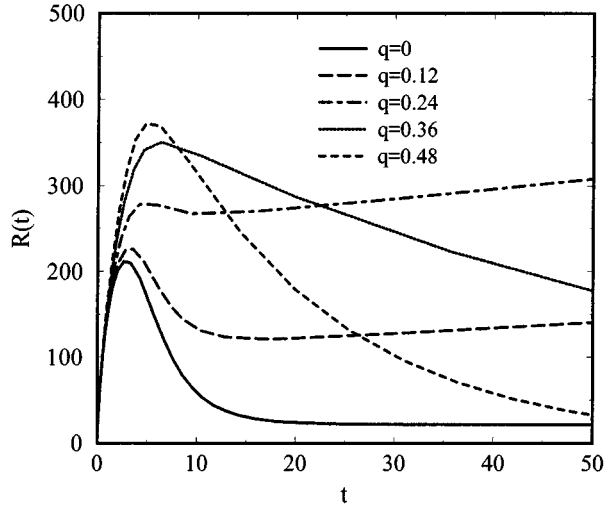

FIG. 8. Transient growth of perturbations for $D=5$ and $b=10^{-3}$. Shown is $R(t)=|g|_{\max}(t)/|g|_{\max}(0)$ for $q=0,0.12,0.24,0.36,0.48$.

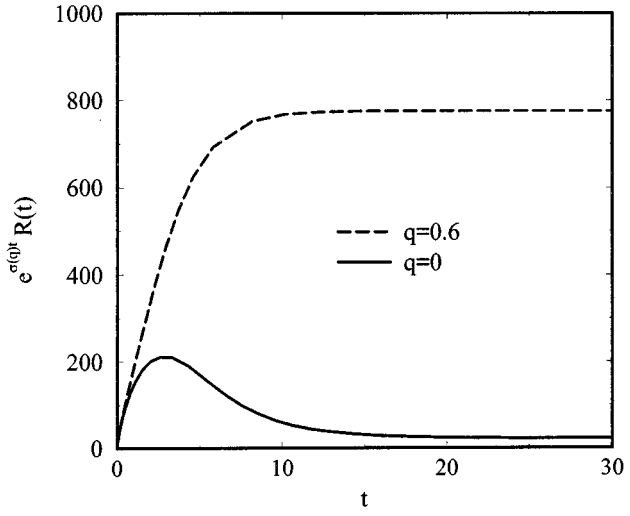

FIG. 9. Transient growth of perturbations for $D=5$ and $b=10^{-3}$. Shown is $R(t)e^{-\beta t}$ for $q=0$ and $q=0.6$.

as t varies. The data shown have $D=5$ and $b=10^{-3}$. We show several different values of q. Note the huge amplification of the solution for early times. Mathematically the transient growth results from the fact that the linear operator in Eq. (11) is not self-adjoint.[34] One can observe this kind of behavior in other hydrodynamic systems, see e.g., Ref. 33.

A useful way to focus on the early time transient is to factor out the exponential behavior as $t\to\infty$. Therefore, for each q, it is useful to examine $R(t)$ divided by $e^{\beta(q)t}$, where $\beta(q)$ is the corresponding eigenvalue (as plotted on the right in Fig. 6). This quantity is shown in Fig. 9 for $q=0$ and 0.6. For linear systems with self-adjoint operators, this ratio decays over time and approaches a constant as $t\to\infty$. However, for non-self-adjoint systems, this ratio could grow by orders of magnitude before saturating. Here there is amplification by a factor of 200 for $q=0$ and 800 for $q=0.6$.

Figure 10 shows how transient growth alone can affect the front. We consider the case $D=5$ and $b=0.01$, for which there is no bump in the profile and hence all growth rates $\beta(q)\leqslant 0$. Nevertheless, transient growth causes perturbations to grow by as much as a factor of 25 on an order one time scale. Consider a perturbation of size $\epsilon=0.01\sim b$. The figure shows the transient growth of a perturbation with wave number $q=0.12$. The top figure shows a contour plot of the front plus perturbation at $t=0$, the bottom graph shows the affect of transient growth alone at $t=4$, when the perturbation has grown to about 0.25. Such amplifications are enough to incite nonlinear effects that can produce finger formation.[21] To verify that the amount of amplification varies *inversely with* b, we show in Fig. 11 the amplification factor as a function of b for $D=0$. The simulations use the same initial perturbation with base profiles corresponding to different values of b. The data depict the $\max_t\max_x|g(x,t)|/\max_x g(x,0)$ for the $q=0$ mode. The numbers indicate that the transient growth is inversely proportional to b, in accordance with the qualitative arguments above. The same scaling is seen upon choosing different values of D and q.

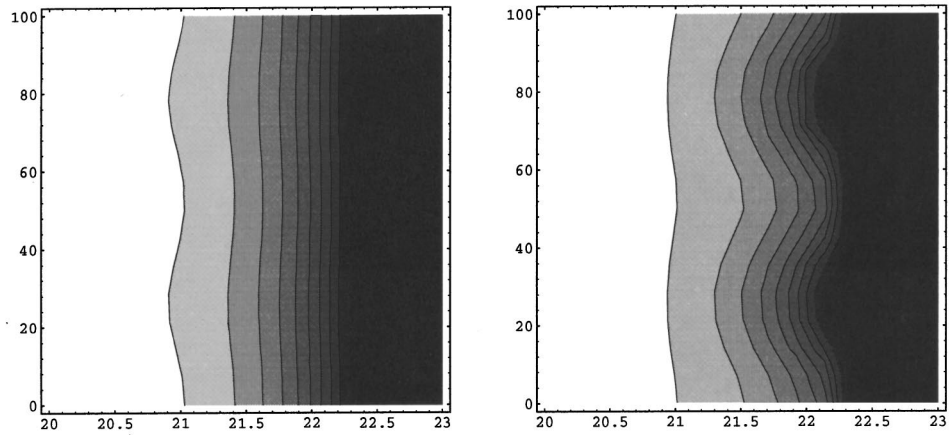

FIG. 10. Contour plot of the thickness profile $h(x,y,t)$ at $D=5, b=0.01$ when all $\beta(q)\leqslant 0$. The figure shows the corrugation of the front by a disturbance of wave number $q=0.12$. In both figures, the color white denotes the thick film ($h=1$), and the color black denotes the thin film region ($h=0.01$). The plot on the top shows a small disturbance placed on the front at time $t=0$. The plot on the bottom shows the linear transient growth of this disturbance at time $t=4$; the maximum of the disturbance has grown by a factor of 25. Such a transient amplification is sufficient to excite nonlinear finger growth.

We emphasize that for experiments amplification of order b^{-1} is precisely what is needed to guarantee instability for spreading on a rough surface. In reality, b is a *local* quantity representing the microscopic length scale at a given point. On a rough surface b *fluctuates* as a function of position. The characteristic amplitude of the fluctuations is also of order b. The surface roughness therefore plays the dual role of both setting the microscopic length scale b *and* providing a natural noise source, with perturbations of order b. Thus, amplification factors of size b^{-1} suffice to amplify these disturbances to be order 1, thereby exciting nonlinearities. A spreading drop on a horizontal surface also experiences amplification of fluctuations on the microscopic scale; however, in this situation there are no nonlinear convective instabilities.

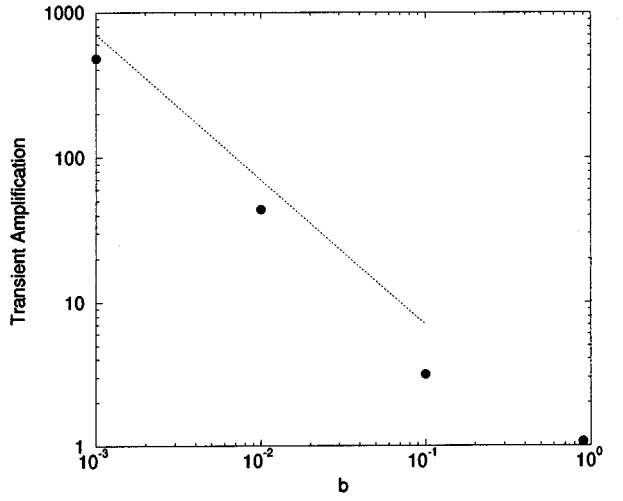

FIG. 11. Transient amplification as a function of b. The dotted line represents the prediction b^{-1}.

B. Experimental consequences

In order for transient modulations of the front of the type shown in Fig. 10 to evolve into fingers, nonlinear effects must cause these corrugations to grow. The predominant nonlinear effect[21,20] is the gravitational forcing in the direction parallel to the inclined plane, given by the $\rho g \sin(\alpha) \times (h^3)_x$ term in Eq. (3). This force causes thicker regions to be convected faster than thin regions, leading to fingers.

The determining factor for finger formation is the time scale of the nonlinear effects compared to the time scale of the linear corrugation (either through transients or modal growth). The latter time scale is

$$\tau_{\text{trans}} = \frac{L}{U_{\text{front}}},$$

where L is a characteristic length of the front and U_{front} is the front velocity.

The time scale for the nonlinear effect follows directly from the convective term in Eq. (3), $\rho g \sin(\alpha)(h^3)_x$, as

$$\tau_{\text{nonlinear}} = \frac{\eta L}{\rho g \sin(\alpha) h_0^2},$$

where h_0 is the characteristic height of the front. When the incline is nearly vertical $\alpha \approx 90°$, then $L=W$ and $h_0=H_N$ as defined above. In this case, the nonlinear time scale is of order the transient time scale since all time scales are of the same order in Eq. (6).

When D is large, the situation is more subtle: The transient growth occurs in the region away from the contact line where $h \sim x(\log(x/b))^{1/3}$. At large D this regime ends a distance of order $\ell_{\text{cap}} = \sqrt{\gamma/(\rho g \cos(\alpha))}$ away from the contact line. Thus, the length scale $L \sim \ell_{\text{cap}}$. The characteristic height $h_0 \sim \theta \ell_{\text{cap}}$, where θ is the macroscopic contact angle.

In order for the nonlinearities to initiate instabilities, it is necessary that $\tau_{\text{trans}} > \tau_{\text{nonlinear}}$. In the $D \to \infty$ limit, the above

estimates imply $U_{\text{front}} < \gamma\theta^2\tan(\alpha)/\eta$. The velocity of the front is given by Tanner's law (8). The condition for an instability is therefore

$$\theta < \tan\alpha \log(1/b) \approx \alpha \log(1/b) \quad \text{as} \quad D \to \infty. \tag{14}$$

In order for the fingers to form at very low inclination angles, the macroscopic contact angle must be *smaller* than a constant multiple of the inclination angle. Therefore, there is a lower critical inclination angle (depending on the drop shape) below which the spreading is perfectly stable: the nonlinearities are insufficient to form fingers from the transient modulations of the front. On the other hand, as long as the macroscopic angle is above this lower critical angle, fingers will form.

V. CONCLUSIONS

This paper revisits the fingering instability of fluid dripping down an inclined plane, first discussed by Huppert.[6] The first part of the paper shows that the fingering instability sometimes happens in experiments even when the base profile is linearly stable. There is a critical inclination angle α^* below which there is linear stability.

We present a solution to this paradox by pointing out that even when the profile is linearly stable, there is always significant transient growth in which small perturbations near the contact line can grow by a factor of 10^3–10^4. The transient growth is a result of the singular dependence of the outer flow on the microscopic scale at the contact line. For example, as the fluid flows across a rough surface, fluctuations in the microscopic scale translate into large fluctuations in the outer flow. This transient growth triggers nonlinearities that result in a fingering instability. The wavelength of the instability is set by the width W of the steady profile. At low inclination angles, this width is significantly larger than for vertical walls. We also reemphasize that regardless of whether the angle is above or below the critical angle for linear instability, transient growth always occurs with amplification inversely proportional to the microscopic length scale at the contact line. There is a second critical inclination angle below which the nonlinearities are not strong enough to trigger finger formation from the transients. Below this inclination angle (which depends on the macroscopic contact angle of the fluid) no fingering occurs.

At inclination angles where the front is linearly stable but fingering still occurs, transient growth causes corrugations of the front. Experiments of de Bruyn clearly show that after an initial transient time period (roughly $t=25$ in dimensionless units) finger growth actually becomes exponential in time.[9] This exponential growth is due to a *nonlinear* effect, explained through a simple geometric argument in Ref. 21.

Analogues of the critical inclination angle can be extended to other coating processes, such as fluid driven by centrifugal forcing. The parameter range explored in published centrifugal experiments is outside the range where our analysis predicts linear stability with transient growth. However, repeating the same arguments as above shows that when the rotation rate is small enough that the ''gravitational flattening'' term is the same order of magnitude as the centrifugal force, stabilization of the profile results. The characteristic rotation rate for this stable regime is $\sqrt{g h_0/R_0^2}$, where R_0 is the radial extent of the drop, h_0 is the characteristic height, and g is the gravitational acceleration. For typical experimental parameters, the critical frequency is of order 1 Hz, which has not been systematically explored. Melo, Joanny, and Fauve[10] note, however, that when the solid substrate is coated with a thick enough film of liquid, the instability is suppressed.

Finally, contact line amplification suggests a natural explanation for irregularity observed in fingering, in which wavelengths of successive fingers vary by as much as 25 percent. This mechanism operates with comparable strength for all wavelengths near the characteristic width W of the profile. For a transient time (of order the experimental time scale) perturbations with wavelength larger than W all amplify at similar rates. Nonlinearities then dictate the wavelength distribution of the experiments. This idea can be tested experimentally: Varying b (the ratio of the outer scale to the inner one) changes the importance of transient effects: Preliminary experiments by Cazabat show for thermal forcing (where a linear instability exists) the distribution of wavelengths broadens as b decreases.[38] For the inclined plane, the distribution of wavelengths should become broader at small inclination angles: this trend has been noted in experiments of Silvi and Dussan,[7] and is also apparent in de Bruyn's data.

The most vexing theoretical problem remaining is to predict the distribution of finger wavelengths as a function of b and the inclination angle. In experiments, the microscopic length scale b is *not* constant, but fluctuates as a function of position: $b(x,y) = \bar{b} + \eta(x,y)$, where $\bar{b}$ is the average microscopic scale and η is a Gaussian noise source. For a particular noise source, what is the distribution of finger wavelengths? For industrial applications, it would be interesting to know whether a function $b(x,y)$ exists for which the fingering instability is actually *suppressed*. In such a situation, the surface could be ''primed'' to suppress instabilities in a driven coating process.

ACKNOWLEDGMENTS

We thank Professor J. de Bruyn for communicating the values of $D(\alpha)$ in his experiments, Professor G. Homsy for helpful comments on the manuscript, and Professor H. Huppert for a penetrating question about the low inclination angle limit. This research was partially supported by the MRSEC Program of the National Science Foundation under Award No. DMR-9400379. In addition, A.B. is supported by the Mathematical, Information, and Computational Sciences Division subprogram of the Office of Computational and Technology Research, U.S. Department of Energy, under Contract No. W-31-109-Eng-38 and the Office of Naval Research under Contract No. N00014-95-1-0752. M.B. acknowledges an NSF postdoctoral fellowship, and support through the School of Science at MIT.

[1]L. Tanner, ''The spreading of silicone oil drops on horizontal surfaces,'' J. Phys. D **12**, 1473 (1979).
[2]P. G. de Gennes, ''Wetting: Statics and dynamics,'' Rev. Mod. Phys. **57**, 827 (1985).
[3]A. M. Cazabat and M. A. Cohen Stuart, ''Dynamics of wetting: Effects of surface roughness,'' J. Phys. Chem. **90**, 5845 (1986).
[4]L. M. Hocking, ''Sliding and spreading of thin two-dimensional drops,'' Q. J. Mech. Appl. Math. **34**, 37 (1981).
[5]Michael Brenner and Andrea Bertozzi, ''Spreading of droplets on a solid surface,'' Phys. Rev. Lett. **71**, 593 (1993).
[6]H. Huppert, ''Flow and instability of a viscous current down a slope,'' Nature **300**, 427 (1982).
[7]N. Silvi and E. B. Dussan, ''On the rewetting of an inclined solid surface by a liquid,'' Phys. Fluids **28**, 5 (1985).
[8]John M. Jerrett and John R. de Bruyn, ''Finger instability of a gravitationally driven contact line,'' Phys. Fluids A **4**, 234 (1992).
[9]John R. de Bruyn, ''Growth of fingers at a driven three-phase contact line,'' Phys. Rev. A **46**, R4500 (1992).
[10]F. Melo, J. F. Joanny, and S. Fauve, ''Fingering instability of spinning drops,'' Phys. Rev. Lett. **63**, 1958 (1989).
[11]Nathalie Fraysse and George M. Homsy, ''An experimental study of rivulet instabilities in centrifugal spin coating of viscous Newtonian and non-Newtonian fluids,'' Phys. Fluids **6**, 6 (1994).
[12]A. M. Cazabat, F. Heslot, S. M. Troian, and P. Carles, ''Finger instability of thin spreading films driven by temperature gradients,'' Nature **346**, 824 (1990).
[13]J. B. Brzoska, F. Brochard-Wyart, and F. Rondelez, ''Exponential growth of fingering instabilities of spreading films under horizontal thermal gradients,'' Europhys. Lett. **19**, 97 (1992).
[14]S. M. Troian, E. Herbolzheimer, S. A. Safran, and J. F. Joanny, ''Fingering instabilities of driven spreading films,'' Europhys. Lett. **10**, 25 (1989).
[15]L. Hocking, ''Spreading and instability of a viscous fluid sheet,'' J. Fluid Mech. **221**, 373 (1990).
[16]J. A. Moriarty, L. W. Schwartz, and E. O Tuck, ''Unsteady spreading of thin liquid films with small surface tension,'' Phys. Fluids A **3**, 733 (1991).
[17]R. Goodwin and G. M . Homsy, ''Viscous flow down a slope in the vicinity of a contact line,'' Phys. Fluids A **3**, 515 (1991).
[18]Leonard W. Schwartz, ''Viscous flows down an inclined plane: Instability and finger formation,'' Phys. Fluids A **1**, 443 (1989).
[19]L. M. Hocking and M. J. Miksis, ''Stability of a ridge of fluid,'' J. Fluid Mech. **247**, 157 (1993).
[20]M. A. Spaid and G. M. Homsy, ''Stability of Newtonian and viscoelastic dynamic contact angles,'' Phys. Fluids **8**, 460 (1996).
[21]Michael P. Brenner, ''Instability mechanisms at driven contact lines,'' Phys. Rev. E **47**, 4597 (1993).
[22]H. P. Greenspan, ''On the motion of a small viscous droplet that wets a surface,'' J. Fluid Mech. **84**, 125 (1978).
[23]Patrick J. Haley and Michael J. Miksis, ''The effect of the contact line on droplet spreading,'' J. Fluid Mech. **223**, 57 (1991).
[24]L. M. Hocking, ''Rival contact-angle models and the spreading of drops,'' J. Fluid. Mech. **239**, 671 (1992).
[25]E. B. Dussan V and S. Davis, ''On the motion of a fluid–fluid interface along a solid surface,'' J. Fluid Mech. **65**, 71 (1974).
[26]E. B. Dussan V, ''The moving contact line: the slip boundary condition,'' J. Fluid Mech. **77**, 665 (1976).
[27]J. de Bruyn, private communication (1995).
[28]Andrea L. Bertozzi, ''Symmetric singularity formation in lubrication-type equations for interface motion,'' SIAM J. Appl. Math. **56**, 681 (1996).
[29]G. Homsy and an anonymous referee pointed out this scenario to us.
[30]L. Landau and E. Lifshitz, *Fluid Mechanics* (Permagon, Oxford, 1987).
[31]Brian F. Farrell and Petros J. Ioannou, ''Variance maintained by stochastic forcing of non-normal dynamical systems associated with linearly stable shear flows,'' Phys. Rev. Lett. **72**, 1188 (1994).
[32]Brian F. Farrell and Petros J. Ioannou, ''Stochastic forcing of the linearized Navier–Stokes equations,'' Phys. Fluids A **5**, 2600 (1993).
[33]K. B. Butler and B. F. Farrell, ''Optimal perturbations and streak spacing in wall bounded shear flow,'' Phys. Fluids A **5**, 774 (1993).
[34]Lloyd N. Trefethen, Anne E. Trefethen, Satish C. Reddy, and Tobin A. Driscoll, ''Hydrodynamic stability without eigenvalues,'' Science **261**, 578 (1993).
[35]D. S. Hennison and S. Reddy, ''On the role of linear mechanisms in transition to turbulence,'' Phys. Fluids A **6**, 1396 (1994).
[36]Jeffrey S. Baggett, Tobin A. Driscoll, and Lloyd N. Trefethen, ''A mostly linear model of transition to turbulence,'' (1996).
[37]L. Boberg and U. Brosa, Z. Naturforsch. A **43**, 697 (1988).
[38]A. M. Cazabat (private communication).